Microwave spectrum, structure, dipole moment, and deuterium nuclear quadrupole coupling constants of the acetylene–sulfur dioxide van der Waals complex

Anne M. Andrews, Kurt W. Hillig II, Robert L. Kuczkowski, A. C. Legon, and N. W. Howard

Citation: The Journal of Chemical Physics **94**, 6947 (1991); doi: 10.1063/1.460228
View online: http://dx.doi.org/10.1063/1.460228
View Table of Contents: http://scitation.aip.org/content/aip/journal/jcp/94/11?ver=pdfcov
Published by the AIP Publishing

Microwave spectrum, structure, dipole moment, and deuterium nuclear quadrupole coupling constants of the acetylene–sulfur dioxide van der Waals complex

Anne M. Andrews, Kurt W. Hillig II, and Robert L. Kuczkowski
Department of Chemistry, University of Michigan, Ann Arbor, Michigan 48109

A. C. Legon and N. W. Howard
Department of Chemistry, University of Exeter, Exeter, Great Britain EX4 4QD

(Received 12 October 1990; accepted 20 February 1991)

Thirty-three *a*- and *c*-dipole transitions of the acetylene–SO_2 van der Waals complex have been observed by Fourier transform microwave spectroscopy and fit to rotational constants $A = 7176.804(2)$ MHz, $B = 2234.962(1)$ MHz, $C = 1796.160(1)$ MHz. The complex has C_s symmetry with the C_2H_2 and SO_2 moieties both straddling an *a*–*c* symmetry plane (i.e., only the S atom lies in the plane). The two subunits are separated by a distance $R_{cm} = 3.430(1)$ Å and the C_2 axis of the SO_2 is tilted 14.1(1)° from perpendicular to the R_{cm} vector, with the S atom closer to the C_2H_2. The dipole moment of the complex is 1.683(5) D. The deuterium nuclear quadrupole hyperfine structure was resolved for several transitions in both $C_2HD\cdot SO_2$ and $C_2D_2\cdot SO_2$. A lower limit for the barrier to internal rotation of the C_2H_2 was estimated to be 150 cm^{-1} from the absence of tunneling splittings. The binding energy was estimated by the pseudo-diatomic model as 2.1 kcal/mol. A distributed multipole analysis was investigated to rationalize the structure and binding of the complex.

INTRODUCTION

Studies of the structure and dynamics of weakly bound molecular complexes can provide insight into the molecular interactions that give rise to chemical and physical properties. To ascertain the principles that govern such interactions, the investigation of a series of related complexes has been extremely valuable.[1] We recently reported on the ethylene·SO_2($C_2H_4\cdot SO_2$) van der Waals complex.[2] To explore the similarities and differences that occur with changes in the hydrocarbon moiety, we undertook a study of the acetylene·SO_2($C_2H_2\cdot SO_2$) complex.

The $C_2H_2\cdot SO_2$ complex was first observed by Muenter and co-workers in a molecular beam mass spectrometry focusing experiment.[3] From the competition for formation among $C_2H_2\cdot SO_2$, $(C_2H_2)_2$, and $(SO_2)_2$, they inferred that a relatively strong van der Waals interaction occurred between C_2H_2 and SO_2. No attempt was made to observe the spectrum and consequently no information on the structure or internal dynamics of the complex was obtained. Studies have shown that SO_2 forms charge-transfer complexes with electron donors such as olefins[4] and aromatic systems,[5] however the acetylene·SO_2 system apparently has not been the subject of such investigations.

We were uncertain of what to expect for the structure of this complex. The $C_2H_4\cdot SO_2$ complex,[2] and similarly the $C_2H_4\cdot O_3$ and $C_2H_2\cdot O_3$ complexes,[6,7] have a stacked near-parallel planes structure. It appears that the primary interaction in $C_2H_4\cdot SO_2$ occurs between the S atom of the SO_2 and the π system of the hydrocarbon. This is consistent with inferences from earlier charge-transfer studies[4] and with a simple distributed multipole electrostatic model.[2] However, the hydrogens of C_2H_2 are considerably more acidic than those of C_2H_4 (Ref. 8) and complexes of acids with SO_2, such as $SO_2\cdot HCl$ and $SO_2\cdot HF$,[9] are characterized by hydrogen bonding of the acid to an O atom of SO_2. The question arises whether this interaction might dominate. Regarding internal dynamics, it was anticipated that the spectrum of the complex might display evidence of internal rotation, especially if its configuration resembled that of the $C_2H_4\cdot SO_2$, $C_2H_4\cdot O_3$, and $C_2H_2\cdot O_3$ complexes. The spectra of the latter all are characterized by tunneling splittings from an internal rotation of the hydrocarbon subunit about an axis nearly collinear with the $R_{c.m.}$ vector. Additionally, the structurally-unrelated acetylene dimer exhibits complicated internal motions which manifest themselves in its infrared and microwave spectra.[10]

This paper reports an analysis of the rotational spectrum of the $C_2H_2\cdot SO_2$ complex which is consistent with the stacked structure. Surprisingly, no evidence for a tunneling motion was detected. The distributed multipole model of Buckingham and Fowler[11,12] was explored to rationalize the structure and binding energy of the $C_2H_2\cdot SO_2$ system; it suggests that there is an electrostatic minimum at the observed conformation with a sizeable stabilization energy, but that there is a second minimum for the *cis* hydrogen bonded structure with a greater electrostatic stabilization energy. Transitions arising from this form have not been assigned, although some residual transitions remain unaccounted for in our study.

EXPERIMENT

Instrument. The rotational transitions of $C_2H_2\cdot SO_2$ were observed in the Fourier transform microwave (FTMW) spectrometer at the University of Michigan using

 0021-9606/91/116947-09$03.00

a modified Bosch fuel injector as a pulsed supersonic nozzle source;[13] initial searches were made on a similar instrument at the University of Exeter.[14] Line widths for transitions not split by deuterium nuclear quadrupole coupling were typically 20 kHz full width at half maximum and center frequencies were reproducible to $\pm$ 2–3 kHz. For the deuterated species, the nuclear quadrupole hyperfine structure was resolved in only a small number of the observed transitions, so the center frequencies were estimated as the most intense of the unresolved hyperfine peaks. These lines were very broad (in some cases up to 150 kHz) and center frequencies were estimated to be accurate only to $\pm$ 20–30 kHz.

The spectrometer was fitted with steel mesh plates for the measurement of Stark effects. The details have been described previously.[15] The electric field was calibrated on each day that Stark effects were measured using the 2_{02}–1_{11}, $M_J = 0$ and $\pm$ 1 transitions of SO_2.[16]

Samples. The spectra were observed with a gas mixture of 1% C_2H_2, 1% SO_2, and 98% Ar at a total backing pressure of 1–2 atm. The C_2D_2 sample (98%) was purchased from MSD Isotopes and used without dilution. The C_2HD sample was prepared by reacting a 70:30 mixture of D_2O/H_2O with CaC_2. The gases evolved were passed through a dry ice trap to remove any remaining water and the acetylene was collected in a liquid nitrogen trap. (The trapping of small amounts of acetylene did not appear to be hazardous.) This produced a mixture of approximately 2:1:1 C_2HD:C_2H_2:C_2D_2. The $S^{18}O^{16}O$ sample was prepared by mixing equal amounts of $S^{16}O_2$ and $S^{18}O_2$ (Alfa Products, 99% ^{18}O) in a glass bulb. Immediately upon mixing, the sample exchanged to give an approximately 2:1:1 mixture of $S^{18}O^{16}O$:$S^{16}O_2$:$S^{18}O_2$. The $C_2H_2 \cdot {}^{34}SO_2$ spectrum was observed in natural abundance (4%).

RESULTS AND ANALYSIS

Spectrum of $C_2H_2 \cdot SO_2$

In the initial search of the region from 8.5 to 12.5 GHz 17 transitions were observed which required both C_2H_2 and SO_2 to be seen. With the aid of Stark effects, eight were assigned as the $C_2H_2 \cdot SO_2$ dimer. The remaining nine lines are believed to arise from another structural isomer of the dimer

TABLE I. Rotational transitions of acetylene·SO_2 (MHz).

	$C_2H_2 \cdot SO_2$		$C_2H_2 \cdot S^{18}O^{16}O$		$C_2HD \cdot SO_2$		$C_2D_2 \cdot SO_2$		$C_2H_2 \cdot {}^{34}SO_2$	
	ν_{obs}	$\Delta\nu$	ν_{obs}	$\Delta\nu$	ν_{obs}	$\Delta\nu$	ν_{obs}	$\Delta\nu$	ν_{obs}	$\Delta\nu$
1_{10}–0_{00}[a]	9 411.619	−2	9 079.281	1	9 099.849	−2	8 786.862	9	9 368.132	−12
2_{11}–1_{01}	13 881.003	0	13 502.197	−2	13 460.696	4	13 048.453	17	13 801.226	11
3_{12}–2_{02}							17 537.228	1		
4_{04}–3_{12}	9 251.510	1	9 246.171	−1	9 034.997	2	8 844.597	29	9 187.032	−1
5_{05}–4_{13}	11 935.979	−2	11 815.592	0	11 610.607	−2				
6_{06}–5_{14}	14 130.081	−3	13 873.924	0	13 694.845	1				
7_{07}–6_{15}	15 807.753	2								
2_{21}–2_{11}	14 825.595	2	13 967.980	0	14 215.982	−25	13 575.007	−19		
3_{22}–3_{12}	14 184.888	4	13 315.746	−1	13 580.769	−12	12 942.311	−12		
4_{23}–4_{13}	13 344.347	2	12 461.449	1	12 748.032	44	12 113.581	9		
5_{24}–5_{14}	12 319.228	0	11 422.369	−1	11 733.450	−17	11 105.514	6		
6_{25}–6_{15}	11 132.961	−1	10 225.288	0			9 944.037	−42		
7_{26}–7_{16}	9 819.733	−3								
8_{27}–8_{17}	8 426.488	2								
2_{20}–2_{12}	16 169.819	0	15 341.822	0	15 551.235	−3	14 908.089	7		
3_{21}–3_{13}	16 954.977	−3	16 153.114	4	16 334.938	6	15 695.350	14		
4_{22}–4_{14}			17 379.871	−3	17 515.650	6				
5_{14}–4_{22}	7 357.151	3	7 930.124	0						
6_{15}–5_{23}	11 981.716	−1								
7_{16}–6_{24}	16 361.052	0								
2_{12}–1_{11}	7 622.854	2	7 503.124	1	7 415.457	10			7 574.372	−9
2_{12}–1_{01}	8 033.840	2	7 920.225		7 822.446	7	7 624.937	−8	7 978.281	13
2_{11}–1_{10}	8 500.363	1	8 398.499	2	8 286.493	14	8 089.045	5	8 435.764	−16
3_{13}–2_{12}	11 416.987	1	11 235.740	−1	11 105.477	1	10 811.980	−9	11 344.847	−1
3_{03}–2_{02}	11 981.219	−1	11 803.970	−1	11 662.409	3	11 363.434	−6	11 900.229	2
3_{22}–2_{21}	12 091.228	0	11 925.042	−3	11 775.427	4	11 481.036	3		
3_{21}–2_{20}	12 202.147	0	12 047.027	−2	11 889.129	−40	11 599.232	−11		
3_{12}–2_{11}	12 731.937	0	12 577.279	1	12 410.644	−5	12 113.719	−18	12 635.765	1
4_{14}–3_{13}	15 191.898	1	14 947.437	1	14 775.893	5	14 383.491	−4		
4_{04}–3_{03}	15 849.392	0	15 601.456	1	15 421.489	−2	15 018.355	−1	12 745.514	−3
4_{23}–3_{22}	16 099.084	2	15 875.337	0	15 677.488	6	15 284.099	4		
4_{32}–3_{31}	16 171.716	1	15 955.212	3	15 752.488	−7				
4_{31}–3_{30}	16 178.374	5	15 963.109	1						
4_{22}–3_{21}	16 371.571	−2	16 174.198	−2	15 956.612	11	15 573.722	4		
4_{13}–3_{12}	16 939.618	−3	16 729.636	0	16 510.270	−5	16 112.841	−3		
5_{15}–4_{14}							17 930.746	−8		

[a]Quantum numbers are J, $K_{prolate}$, K_{oblate}.

[b]$\Delta\nu = \nu_{obs} - \nu_{calc}$ in kHz, where ν_{calc} is obtained from the constants in Table II.

TABLE II. Spectroscopic constants for acetylene·SO_2.[a]

	$C_2H_2\cdot SO_2$	$C_2H_2\cdot S^{18}O^{16}O$	$C_2HD\cdot SO_2$	$C_2D_2\cdot SO_2$	$C_2H_2\cdot{}^{34}SO_2$
A/MHz	7176.804(2)[b]	6867.696(2)	6919.318(15)	6655.943(10)	7151.505(17)
B/MHz	2234.962(1)	2211.727(1)	2180.661(3)	2131.012(2)	2216.789(10)
C/MHz	1796.160(1)	1763.992(1)	1745.100(3)	1696.556(2)	1786.069(8)
D_J/kHz	7.617(3)	7.363(5)	7.24(7)	7.00(6)	7.1(1)
D_{JK}/kHz	42.19(2)	42.45(2)	34.4(2)	28.7(3)	41.1(18)
D_K/kHz	−42.6(4)	−43.1(3)	−33(3)	−40.0(2)	43.0[c]
d_1/kHz	−1.681(1)	−1.691(3)	−1.63(3)	−1.66(3)	−0.8(3)
d_2/kHz	−0.354(1)	−0.375(2)	−0.33(3)	−0.25(3)	1.0[c]
n[d]	33	29	26	24	10
$\Delta\nu_{rms}$/kHz[e]	2	2	17	13	15

[a] Watson S reduction, I^r representation.
[b] Uncertainties represent one standard deviation in the least-squares fit.
[c] Parameter fixed in least-squares fit.
[d] Number of transitions in the fit.
[e] $\Delta\nu = \nu_{obs} - \nu_{calc}$.

or a trimer species. Attempts to fit these transitions have been unsuccessful. Following the initial assignment, a total of 33 a- and c-dipole transitions arising from levels up to $J = 8$ and $K_p = 3$ were observed in the region 7–18 GHz. These are listed in Table I. The transitions were fit to a Watson S-reduced Hamiltonian using the I^r representation.[17] The derived spectroscopic constants are listed in Table II.

The spectra of $C_2D_2\cdot SO_2$, $C_2HD\cdot SO_2$, $C_2H_2\cdot S^{18}O^{16}O$, and $C_2H_2\cdot{}^{34}SO_2$ were also observed. These were fit to the same Watson Hamiltonian and their transitions and spectroscopic constants are listed in Tables I and II, respectively.

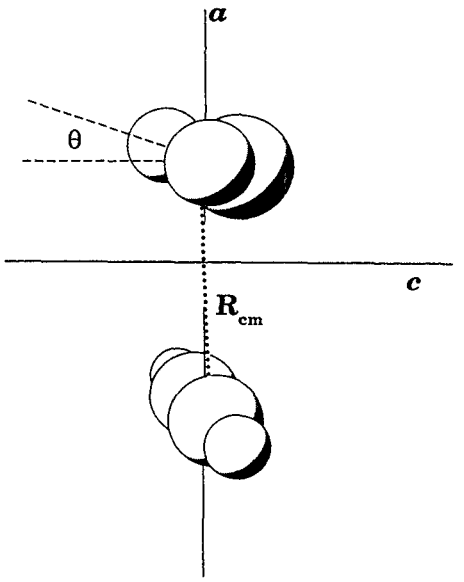

FIG. 1. The acetylene·SO_2 coordinate system and geometry. $R_{c.m.}$ is the distance between the centers of mass of the acetylene and SO_2. θ is the tilt angle between the C_2 axis of SO_2 and the perpendicular to the $R_{c.m.}$ vector, with clockwise rotation defined as positive.

Structure

The small difference in the planar second moment P_{bb} (Ref. 18) for $C_2H_2\cdot SO_2$ (62.8303 amu·Å^2) and $C_2H_2\cdot{}^{34}SO_2$ (62.8228 amu·Å^2) places the S atom in the a–c plane. A comparison of P_{bb} of the $C_2H_2\cdot SO_2$ complex (62.8303 amu·Å^2) with the sum of P_{aa} of free acetylene[19] and P_{aa} of free SO_2 (Ref. 19) (14.2352 + 48.7828 = 63.0180 amu·Å^2) indicates that the two subunits both straddle an a–c symmetry plane, with the C_2 axis of the SO_2 rotated 90° to the C_∞ axis of the acetylene, as shown in Fig. 1. With this orientation established, the structure of the $C_2H_2\cdot SO_2$ complex is defined by the two parameters $R_{c.m.}$ and θ (Fig. 1), where $R_{c.m.}$ is the distance between the centers of mass of the acetylene and SO_2 and θ is the tilt angle between the C_2 axis of the SO_2 and the perpendicular to $R_{c.m.}$. It is assumed that the C_2H_2 and SO_2 subunits retain their uncomplexed geometries.[19]

A least-squares fit of the moments of inertia of the normal isotopic species yielded two structures which had fits of the same quality: both had $R_{c.m.} = 3.43$ Å, but the two had nearly equal and opposite values for θ (+ 14° and − 16°). The isotopic species sensitive to the sign of θ are $C_2H_2\cdot S^{18}O^{16}O$ and $C_2H_2\cdot{}^{34}SO_2$, however addition of their rotational constants to the least-squares fit again produced two structures as shown in Table III. The fit of the structure with the positive angle, where the S atom is nearer the C_2H_2, is of slightly better quality than that of structure with the negative angle, but the difference is not great enough to be conclusive. A more compelling argument for the correct geometry results from the comparison of the a coordinates of the oxygen and sulfur atoms for the two structures to those calculated using Kraitchman's equations,[20] also given in Table III. The Kraitchman coordinates are consistent with the structure labeled I. This structure is similar to the structure of $C_2H_4\cdot SO_2$, where the S atom is also nearer the C_2H_4. The structures calculated for each of the isotopically substituted

TABLE III. Structural parameters from least-squares fits of the moments of inertia of $C_2H_2 \cdot SO_2$, $C_2H_2 \cdot S^{18}O^{16}O$, and $C_2H_2 \cdot {}^{34}SO_2$ and coordinates from Kraitchman substitution calculations.

	I[a]	II[a]	Kraitchman
$R_{c.m.}$/Å	3.431	3.431	
θ/deg[b]	13.9	−16.0	
ΔI_{rms}/amu·Å^2 [c]	0.28	0.50	
a(O)/Å[d]	1.08	0.89	1.04
b(O)/Å[d]	1.23	1.23	1.24
c(O)/Å[d]	0.34	0.36	0.35
a(S)/Å[d]	−0.90	−1.10	0.90
b(S)/Å[d]	0.0	0.0	0.0
c(S)/Å[d]	−0.36	−0.34	0.38

[a] Two least-squares fits of moments of inertia. See the text.
[b] Positive angle indicates clockwise rotation. See Fig. 1.
[c] $\Delta I = I_{obs} - I_{calc}$.
[d] a,b,c coordinate of atom.

species separately,along with that from a least-squares fit of all of the moments of inertia simultaneously, are shown in Table IV.

It is difficult to estimate the accuracy of this structure in relation to a physically well-defined average or equilibrium structure. The large amplitude vibrations of a floppy molecule certainly contaminate the moments of inertia from which the structure is derived. This is most easily seen in the discrepancy between the observed value of P_{bb} and the one calculated from the structures of C_2H_2 and SO_2. However, this difference of 0.19 amu·Å^2 is not as large as in $C_2H_4 \cdot SO_2$ (1.33 amu·Å^2) and other complexes. Also, a comparison of the structures calculated for each isotopic species shows that there is very little change upon isotopic substitution. Because the moments of inertia of each isotopic species will be contaminated differently due to changes in vibrational amplitudes, this suggests that the effects of vibrational averaging are not so apparent in this complex. It therefore seems reasonable to estimate that the average structure (so-called r_0)[21] is within ± 0.03 Å for $R_{c.m.}$ and ± 5° for θ.

Dipole moment

The dipole moment of the complex was determined by measuring the Stark effect of nine transitions and fitting the observed Stark shifts using a least-squares procedure. Owing to the symmetry of the complex, it was expected that μ_b would be identically zero. To test this, μ_b was initially allowed to vary in the fit. This resulted in $\mu_b^2 = 0.01 \pm 0.09D^2$, consistent with μ_b equal to zero. Therefore, in the final fit shown in Table V, μ_b was constrained to zero. This resulted in a total dipole moment of $1.683(5)D$, with components $|\mu_a| = 0.721(2)D$ and $|\mu_c| = 1.521(5)D$.

It is interesting that the dipole moment of the $C_2H_2 \cdot SO_2$ complex ($1.683D$) is quite similar to the dipole moment of free SO_2 ($1.633D$).[16] However, the dipole moment of the complex is rotated some 14° from the C_2 axis of the SO_2 subunit. (The direction of the dipole moment of the complex is selected such that it is dominated by the permanent dipole moment of SO_2.) If the dipole moment of SO_2 is projected onto the principal axes of the complex using the structure determined above, the components are estimated to be $\mu_a = 0.395D$ and $\mu_c = -1.584D$. A positive sign implies that the component points along the positive axis in Fig. 1. To explore whether the discrepancy between the projections and the observed components can be explained by polarization, we employed a simple model in which the acetylene was treated as a point polarizability at its center of mass with components $\alpha_{\parallel} = 4.86$ Å^3 and $\alpha_{\perp} = 2.94$ Å^3.[22] A GAUSSIAN86 (Ref. 23) calculation was undertaken (HF/6-31G*) to estimate the electric field from free SO_2 at the site of the center of mass of the acetylene. From this electric field, induced dipole components of $\mu_a = 0.342D$ and $\mu_c = 0.118D$ were calculated for acetylene. The same approach was used to estimate the dipole moment induced in the SO_2 by the acetylene. From the calculated electric field from acetylene and SO_2 polarizability components $\alpha_{aa} = 5.32$ Å^3, $\alpha_{bb} = 3.51$ Å^3 and $\alpha_{cc} = 3.01$ Å^3,[24] components of $\mu_a = 0.181D$ and $\mu_c = -0.031D$ were calculated for SO_2. The total induced dipole components $\mu_a = 0.521D$ and $\mu_c = 0.087D$ compare favorably with the difference between the experimental and projected values, which gives components $\mu_a = 0.326D$ and $\mu_c = 0.063D$. If the same calculation is performed for the angle $\theta = -14°$, components $\mu_a = 0.2D$ and $\mu_c = 0.2D$ are obtained, providing further evidence that the sign of the angle θ is positive.

Deuterium nuclear quadrupole coupling

The hyperfine structure from deuterium nuclear quadrupole coupling was resolved and assigned for several transitions in both $C_2HD \cdot SO_2$ and $C_2D_2 \cdot SO_2$. Quadrupole

TABLE IV. Structure of $C_2H_2 \cdot SO_2$ from individual fits of the moments of inertia for each isotopic species.

	$C_2H_2 \cdot SO_2$	$C_2HD \cdot SO_2$	$C_2D_2 \cdot SO_2$	$C_2H_2 \cdot S^{18}O^{16}O$	$C_2H_2 \cdot {}^{34}SO_2$	All species
$R_{c.m.}$/Å	3.431(1)[b]	3.429(2)	3.426(2)	3.430(2)	3.432(2)	3.430(1)
θ/deg	13.9(1)	14.1(1)	14.2(1)	14.0(1)	13.9(1)	14.1(1)
ΔI_{rms}^{a}/amu Å^2	0.315	0.316	0.319	0.312	0.314	0.353

[a] $\Delta I = I_{obs} - I_{calc}$.
[b] Uncertainties represent one standard deviation in the least-squares fit.

TABLE V. Stark coefficients $(\Delta\nu/\epsilon^2)$[a] and dipole moment of $C_2H_2\cdot SO_2$.

	$\|M\|$	obs	o–c[b]
2_{02}–1_{01}	1	33.97	0.28
2_{12}–1_{11}	0	6.22	−0.04
2_{12}–1_{11}	1	56.32	−0.75
2_{11}–1_{10}	1	−60.76	−0.81
1_{10}–0_{00}	0	31.33	0.13
2_{11}–1_{01}	1	38.40	−0.23
4_{04}–3_{12}	0	7.44	0.02
4_{04}–3_{12}	2	−13.27	0.21
4_{04}–3_{12}	3	−39.50	0.13
$\mu_a = 0.721(2)D$	$\mu_c = 1.521(5)D$	$\mu_t = 1.683(5)D$	

[a] Second order Stark effect in MHz/(kV/cm)^2.
[b] Stark coefficients calculated using rotational constants listed in Table II.

coupling constants are determined from a least-squares fit of the hyperfine components treating the quadrupole interaction as a perturbation on the rotational energy.[25] The fit of $C_2HD\cdot SO_2$ is shown in Table VI. The quadrupole coupling constants for both $C_2HD\cdot SO_2$ and $C_2D_2\cdot SO_2$ are shown in Table VII. Also included in Table VII are quadrupole coupling constants that have been determined for C_2HD and C_2D_2 in previous studies.[26–31]

It should be noted that the labels $\chi_{aa}, \chi_{bb}, \chi_{cc}$ are strictly correct only for the $C_2H_2\cdot SO_2$ complexes. The observed χ's for C_2HD, C_2D_2, and $C_2D_2\cdot Ar$ have been relabeled so that χ_{bb} corresponds to the field gradient along the C–D bond axis for all species to facilitate discussion. For the values determined from the excited bending vibrational states of acetylene, this appears to be a good approximation.

The first point to make is that for $C_2H_2\cdot SO_2$ $q_{aa} = q_{cc} = -0.5q_{bb}$ (within experimental uncertainty). Although the location of the principal axis of the quadrupole tensor is not known, this relationship between the observed q's, as well as the geometric arrangement of the complex, suggests that the gradient along the C–D bond is nearly cylindrically symmetric. Secondly, the scatter in the values in Table VII does not provide a very clear-cut reference point for χ_D. This makes it difficult to estimate how greatly the electric field gradient at the D site has been affected by complexation to SO_2, except to suggest that any effect must be 10% or less.

To explore the effect of complexation more quantitatively, GAUSSIAN86 was used to estimate whether the electric field gradient of the SO_2 moiety will directly affect the coupling constant of the D. The field gradient produced by free SO_2 at the position of the D in the complex was calculated with both the GAUSSIAN 6-31G* and 4-31G basis sets and indicated a negligible contribution of $\leqslant$0.003 MHz to the coupling constant. The calculated value for free acetylene in the 6-31G* basis set was $\chi_{\|} = -0.128$ MHz and $\chi_{\perp} = 0.256$ MHz, in reasonable agreement with the observed values, but considerably poorer than the literature value in Table VII, for which a larger basis set was employed. Of course, this calculation does not estimate whether an electronic perturbation of the acetylene by the SO_2 can affect the field gradient at the D site. When a supermolecule calculation (HF/6-31G*) is performed for the $C_2H_2\cdot SO_2$ complex,

TABLE VI. Deuterium nuclear quadrupole splitting in $C_2HD\cdot SO_2$ (MHz).

J'	K'_p	K'_0	F'	J''	K''_p	K''_0	F''	ν_{obs}	$\Delta\nu$[a]
1	1	0	1	0	0	0	1	9099.822	0.002
1	1	0	2	0	0	0	1	9099.849	0.000
1	1	0	0	0	0	0	1	9099.892	−0.002
3	2	2	2	2	2	1	1	11 775.425	0.004
3	2	2	4	2	2	1	3	11 775.401	−0.002
3	2	2	3	2	2	1	2	11 775.368	−0.003
2	1	1	1	1	0	1	1	13 460.761	−0.001
2	1	1	3	1	0	1	2	13 460.701	0.005
2	1	1	2	1	0	1	1	13 460.622	−0.001
2	1	1	2	1	0	1	2	13 460.629	−0.003
3	2	2	3	3	1	2	3	13 580.837	0.001
3	2	2	4	3	1	2	4	13 580.762	−0.001
3	2	2	2	3	1	2	2	13 580.738	0.000
2	0	2	1	1	0	1	1	7822.490	−0.002
2	0	2	3	1	0	1	2	7822.447	0.000
2	0	2	1	1	0	1	0	7822.419	0.002
2	1	2	1	1	1	1	0	7415.526	−0.001
2	1	2	2	1	1	1	2	7415.487	0.000
2	1	2	3	1	1	1	2	7415.457	0.001
2	1	2	2	1	1	1	1	7415.429	0.002
2	1	2	1	1	1	1	1	7415.377	−0.002
2	1	1	1	1	1	0	1	8286.557	−0.001
2	1	1	3	1	1	0	2	8286.494	0.001
2	1	1	2	1	1	0	1	8286.459	0.000

[a] $\Delta\nu = \nu_{obs} - \nu_{calc}$ where ν_{calc} was obtained with the constants in Table VII.

TABLE VII. Deuterium nuclear quadrupole coupling constants (MHz) for C_2H_2 and C_2H_2-containing complexes.

	χ_{aa}	χ_{bb}	χ_{cc}	Method	Ref.
$C_2HD{\cdot}SO_2$	−0.101(3)	0.198(3)	−0.097(3)	FTMW	
$C_2D_2{\cdot}SO_2$	−0.098(4)	0.199(7)	−0.101(4)	FTMW	
$C_2D_2{\cdot}Ar$		0.2044(10)		MBER	27
C_2D_2		0.225(30)		MBMR	28
C_2HD		0.231		*ab initio*	29
C_2D_2/C_2HD		0.1986(7)		NMR	30
		χ_{bb}	$\chi_{aa}-\chi_{cc}$		
C_2HD $v_4=1$		0.221(2)	−0.006(4)	MBER	31
C_2HD $v_5=1$		0.207(6)	−0.031(22)	MBER	31
C_2D_2 $v_4=1$		0.20916		MBER	32
C_2D_2 $v_5=1$		0.20870		MBER	32

$\chi_{aa}=0.127$, $\chi_{bb}=-0.255$, and $\chi_{cc}=0.128$ are obtained. Although these coupling constants are not very accurate, their similarity to those calculated above for free acetylene indicates that SO_2 does not introduce a significant perturbation of the electric field gradient at the deuterium in the complex.

The contrast between the small or negligible electronic perturbation effects on $(eqQ)_D$ in acetylene upon complexation compared to the larger polarization effects indicated by the dipole moment data is striking. One possible resolution of this paradox is that considerable polarization of the acetylene occurs, but that it is confined primarily to the C≡C triple bond while the C–H bonds are relatively unaffected. Another possibility is that the electron density in the C–H bond is affected more significantly but in a manner that does not markedly alter the electric field gradient at the deuterium site. It is difficult to choose between these alternatives.

Internal rotation

Recent studies of $C_2H_4{\cdot}SO_2$ (Ref. 2), $C_2H_2{\cdot}O_3$ (Ref. 6), and $C_2H_4{\cdot}O_3$ (Ref. 7) have shown that all three complexes have an internal motion that splits their rotational transitions into tunneling doublets. It has been shown in $C_2H_4{\cdot}SO_2$ that the motion is an internal rotation of the hydrocarbon about the axis perpendicular to its plane and hindered by a V_2 barrier of about 30 cm^{-1}. The same motion has been postulated for $C_2H_2{\cdot}O_3$ and $C_2H_4{\cdot}O_3$. It was expected, therefore, that the structurally similar $C_2H_2{\cdot}SO_2$ complex would also exhibit internal rotation splittings. Spectra were predicted for barriers between $V_2=0$ and 30 cm^{-1} using the internal rotation Hamiltonian applied to the $C_2H_4{\cdot}SO_2$ problem.[32] Extensive searches in the predicted regions produced a number of lines with low-J second order Stark effects which required both C_2H_2 and SO_2, but the Stark effects and patterns were inconsistent with the predicted spectra. We have concluded that these unassigned transitions belong to one or more structural isomers of the $C_2H_2{\cdot}SO_2$ complex and/or a trimer species.

Additional insights were obtained from the quadrupole coupling patterns of the $C_2D_2{\cdot}SO_2$ species. If the $C_2H_2{\cdot}SO_2$ complex were undergoing an internal rotation similar to that observed in $C_2H_4{\cdot}SO_2$, with the acetylene rotating about an axis nearly coincident with the $R_{c.m.}$ vector, equivalent deuterium atoms would be exchanged in $C_2D_2{\cdot}SO_2$. The Pauli principle requires that the symmetry of the rotational (or rotation-tunneling) level be appropriately matched with the symmetry of the nuclear spin function such that the overall wave function is symmetric with respect to interchange of two bosons. For moderate and high barrier problems there is a clear distinction between symmetric and antisymmetric tunneling states. Therefore, if internal rotation occurred, the nuclear quadrupole coupling pattern for a given transition would display only the hyperfine components resulting from either the even or the odd nuclear spin functions, depending on whether the tunneling state was symmetric or antisymmetric. Figure 2 shows the hyperfine pattern of the 1_{10}–0_{00} transition of $C_2D_2{\cdot}SO_2$. Beneath it is a stick diagram of the

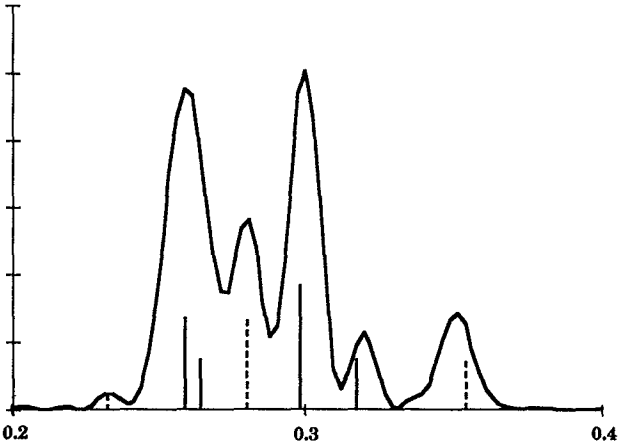

FIG. 2. Power spectrum of the 1_{10}–0_{00} transition of $C_2D_2{\cdot}SO_2$, showing nuclear quadrupole coupling hyperfine structure. The spectrum is the average of 2000 gas pulses with 512 points digitized at a sampling rate of 0.2 μs. In the stick diagram below, the solid lines are the hyperfine components arising from even nuclear spin states, the dashed lines from odd nuclear spin states.

hyperfine transitions with the even nuclear spin components shown in solid lines and the odd in dashed lines. All the hyperfine components are observed, indicating that the complex is not undergoing any internal rotation. This argument can also be applied to the low barrier or free internal rotation situation in which case the assigned transitions would arise from the $m = 0$ nondegenerate state and should also exhibit only one nuclear spin symmetry.

Using the internal rotation Hamiltonian employed in the $C_2H_4 \cdot SO_2$ system,[2,32] a lower limit to the barrier to internal rotation was estimated for the $C_2H_2 \cdot SO_2$ complex. This was obtained by varying the barrier until the largest predicted splittings were below the instrumental resolution. As the observed transitions were very sharp in the normal isotopic species (FWHM was about 20 kHz), a splitting of 5 to 10 kHz was selected for this limit; anything larger would result in broader lines, if not distinct, split peaks. At $V_2 = 135$ cm^{-1}, the largest of the splittings collapsed to < 10 kHz. At $V_2 = 150$ cm^{-1} they were < 5 kHz.

Electrostatic analysis

To determine whether electrostatic interactions may be used to rationalize the structure and internal dynamics of the $C_2H_2 \cdot SO_2$ system, the distributed multipole model of Buckingham and Fowler was explored.[11] The distributed multipoles calculated by Buckingham and Fowler for C_2H_2 and SO_2 were used directly and the van der Waals radii were taken from Pauling.[33] A search of all possible geometries in which the center of mass distance and five angles were varied produced two electrostatic minima. The *cis* hydrogen bonded structure, similar to $SO_2 \cdot HF$ and $SO_2 \cdot HCl$, has the largest stabilization energy (-1600 cm^{-1}), while the stacked structure, similar to the experimental geometry, is at the second minimum (-815 cm^{-1}). This is similar to the result reported for the $SO_2 \cdot HCN$ (Refs. 34 and 35) complex, where initial predictions from the distributed multipole model indicated that the structure would be *cis* hydrogen bonded.[11] However, experimental evidence revealed that the HCN sat perpendicular to the SO_2 plane with the N atom pointed toward the S in an anti-hydrogen bonded configuration. It was only when the N–S distance was permitted to be shorter than the sum of the N and S van der Waals radii, as was determined experimentally, that the distributed multipole model found a global minimum at the experimental structure. In the case of the $C_2H_2 \cdot SO_2$, however, the point of closest contact determined experimentally is not shorter than the hard sphere sums, so we have not explored whether relaxing the hard sphere contact constraint will reverse the stability order of the two isomers. Using the stacked structure, it is interesting to examine whether electrostatics could be used to predict correctly the experimentally determined tilt angle of the SO_2. Figure 3 shows the calculated electrostatic energy as the angle θ is varied from 0 to 90° at the experimental distance, $R_{c.m.} = 3.430$ Å. There is a shallow minimum at $\theta = 10$–20°, consistent with the observed value of 14°.

Finally, it is interesting to compare the interaction energy calculated with the distributed multipole model with that calculated with the pseudo-diatomic model. Using the pseudo-diatomic model of Millen,[36] the force constant is calculated as 0.0497 mdyne/Å from $k_s = 16\pi^4\mu_D^2 R_{c.m.}^2 D_J^{-1} h^{-1} \times [4B^4 + 4C^4 - (B + C)^2(B - C)^2]$. From this the binding energy is determined to be 390 cm^{-1}. The electrostatic energy (815 cm^{-1}) is different by a factor of 2.

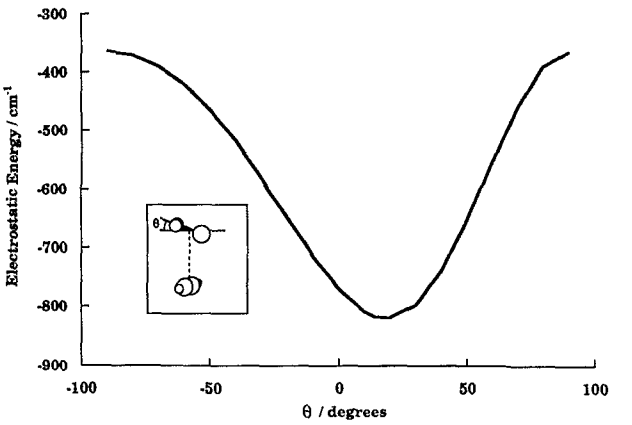

FIG. 3. Electrostatic energy as a function of the tilt angle of SO_2, for $R_{c.m.}$ fixed at the experimental distance.

DISCUSSION

The structure of the $C_2H_2 \cdot SO_2$ complex is similar to that of the $C_2H_4 \cdot SO_2$ complex, with the principal interaction apparently between the S atom of the SO_2 and the π system of the C_2H_2. The $R_{c.m.}$ distance in the $C_2H_2 \cdot SO_2$ is considerably shorter than that in the $C_2H_4 \cdot SO_2$ (3.430 Å vs 3.504 Å). A better comparison is perhaps the distance from the S atom to the center of mass of the hydrocarbon. For $C_2H_2 \cdot SO_2$, this distance is 3.363 Å, where it is 3.438 Å in the $C_2H_4 \cdot SO_2$ complex, the difference being 0.065 Å. When a similar comparison is made for other complexes of C_2H_2 and C_2H_4, as shown in Table VIII, a similar trend is observed.[6,7,37–40] In each case, the $C_2H_2 \cdot X$ distance is shorter than the $C_2H_4 \cdot X$ distance. However, the difference between the C_2H_2 and C_2H_4 distances is considerably greater in the SO_2 complexes than in any of the other complexes.

TABLE VIII. Comparison of acetylene- and ethylene-containing complexes.

	$R_{c.m.}$/Å	$R_{x\ c.m.}$[a]/Å	k_s/mdyn Å^{-1}	ϵ/cm^{-1}
$C_2H_2 \cdot SO_2$	3.430	3.363	0.047	390
$C_2H_4 \cdot SO_2$	3.502	3.438	0.057	490
$C_2H_2 \cdot O_3$	3.251			
$C_2H_4 \cdot O_3$	3.279			
$C_2H_2 \cdot HF$	3.075	3.122		
$C_2H_4 \cdot HF$	3.097	3.144		
$C_2H_2 \cdot HCl$	3.699	3.699	0.069	643
$C_2H_4 \cdot HCl$	3.742	3.724	0.066	627
$C_2H_2 \cdot HCN$	4.216	3.655	0.053	642
$C_2H_4 \cdot HCN$	4.257	3.709	0.046	575

[a] $R_{x-c.m.}$ is distance from center of mass of hydrocarbon to nearest heavy atom.

TABLE IX. *Ab initio* energies for $C_2H_2 \cdot SO_2$ and $C_2H_4 \cdot SO_2$.

	$C_2H_2 \cdot SO_2$	$C_2H_4 \cdot SO_2$
V_2 barrier/cm^{-1}	315	173
Binding energy/cm^{-1}	910	890
MP4 energies/a.u.		
$C_2H_x \cdot SO_2(\phi = 0°)$	− 624.800 8805	− 626.027 6719
$C_2H_x \cdot SO_2(\phi = 90°)$	− 624.799 4467	− 626.026 8841
SO_2	− 547.703 8643	− 547.703 8643
C_2H_x	− 77.092 8886	− 78.319 7521

Also in Table VIII are the binding energies calculated for each complex from the pseudo-diatomic model. Comparison of the $C_2H_2 \cdot SO_2$ and $C_2H_4 \cdot SO_2$ complexes shows that the $C_2H_4 \cdot SO_2$ has the larger binding energy. This is the reverse of the trend shown for the other C_2H_2- and C_2H_4-containing complexes. It is difficult to determine whether this represents some true physical difference between the SO_2-containing complexes and the others or whether it is an artifact. One reason to doubt its validity is that the $C_2H_4 \cdot SO_2$ complex undergoes a tunneling motion which contaminates its rotational and distortion constants. This is particularly apparent in the A and D_K constants, but the D_J constant used in this analysis may be sufficiently contaminated to affect the binding energies calculated.

The most perplexing finding of this study is the observation that the $C_2H_2 \cdot SO_2$ complex does not undergo an internal rotation of the C_2H_2 subunit. It is certainly inconsistent with the series $C_2H_4 \cdot SO_2$, $C_2H_4 \cdot O_3$, $C_2H_2 \cdot O_3$, where the splitting in the 1_{10}–0_{00} transition is 25, 10, and 5 MHz, respectively. Extrapolating, one would expect from chemical intuition that the same transition in the $C_2H_2 \cdot SO_2$ complex would be split by 10–15 MHz. What exactly is giving rise to this difference is unclear.

Ab initio studies were undertaken in an attempt to shed some light on this matter. Geometry optimizations of the parameters $R_{c.m.}$, θ_1, and θ_2 at the Hartree–Fock level were performed on both the $C_2H_2 \cdot SO_2$ and $C_2H_4 \cdot SO_2$ systems for the experimental orientation and for the orientation in which the hydrocarbon subunit is rotated by 90° such that the C–C bond axis of the hydrocarbon is in line with the C_2 axis of the SO_2. At these optimized geometries single point energy calculations were performed at the MP4 level. The difference in energy between the two conformations (Table IX) was used to estimate the V_2 barrier to internal rotation. The calculations indicate that the $C_2H_2 \cdot SO_2$ complex should have a higher barrier to internal rotation by a factor of two, consistent with experiment. Also included in Table IX are estimates of the binding energies, which were calculated by subtracting the energies calculated for the rigid subunits from the total complex energies. Interestingly, the *ab initio* results indicate that the $C_2H_2 \cdot SO_2$ complex is slightly more strongly bound that the $C_2H_4 \cdot SO_2$ complex. This is reversed compared to the pseudo-diatomic calculation, but follows the trend of the HCl and HCN complexes with C_2H_2 and C_2H_4.

The electrostatic calculations suggest that a second isomer of the $C_2H_2 \cdot SO_2$ complex should exist in which the C_2H_2 is hydrogen bonded to the O atom of the SO_2. This would be similar to the complexes of SO_2 with strong acids like HF and HCl. Although a number of additional transitions have been observed, we have been unable to assign them to this isomer.

ACKNOWLEDGMENTS

This work was supported by grants from the National Science Foundation, Washington, DC. We thank Amine Taleb-Bendiab for his assistance with the internal rotation calculations.

[1] A. C. Legon and D. J. Millen, Acc. Chem. Res. **20**, 39 (1987).
[2] A. M. Andrews, A. Taleb-Bendiab, M. S. LaBarge, K. W. Hillig II, and R. L. Kuczkowski, J. Chem. Phys. **93**, 7030 (1990).
[3] J. S. Muenter, R. L. DeLeon, and A. Yokozeki, Faraday Discuss. Chem. Soc. **73**, 63 (1982).
[4] D. Booth, F. S. Dainton, and K. J. Ivin, Faraday Soc. Trans. **55**, 1293 (1959).
[5] (a) L. J. Andrews and R. M. Keefer, J. Am. Chem. Soc. **73**, 4169 (1951); (b) J. R. Grover, E. A. Walters, J. K. Newman, and M. G. White, J. Am. Chem. Soc. **107**, 7329 (1985).
[6] C. W. Gillies, J. Z. Gillies, R. D. Suenram, and F. J. Lovas, J. Am. Chem. Soc. (submitted).
[7] C. W. Gillies, J. Z. Gillies, R. D. Suenram, and F. J. Lovas, Ohio State Molecular Spectroscopy Symposium, 1989, Columbus, OH, Paper TF4.
[8] R. T. Morrison and R. N. Boyd, *Organic Chemistry*, 4th ed. (Allyn and Bacon, Newton, MA, 1983), pp. 566–568.
[9] A. J. Fillery-Travis and A. C. Legon, Chem. Phys. Lett. **123**, 4 (1986).
[10] G. T. Fraser, R. D. Suenram, F. J. Lovas, A. S. Pine, J. T. Hougen, W. J. Lafferty, and J. S. Muenter, J. Chem. Phys. **89**, 6028 (1988).
[11] A. D. Buckingham and P. W. Fowler, Can. J. Chem. **63**, 2018 (1985).
[12] P. A. Kollman, Acc. Chem. Res. **10**, 365 (1977).
[13] K. W. Hillig II, J. Matos, A. Scioly, and R. L. Kuczkowski, Chem. Phys. Lett. **133**, 359 (1987).
[14] A. C. Legon and L. C. Willoughby, Chem. Phys. **74**, 127 (1982).
[15] R. K. Bohn, K. W. Hillig II, and R. L. Kuczkowski, J. Phys. Chem. **93**, 3456 (1989).
[16] F. J. Lovas, J. Chem. Phys. Ref. Data **14**, 395 (1985).
[17] J. K. G. Watson, J. Chem. Phys. **46**, 1935 (1967).
[18] $P_{bb} = 0.5(I_a + I_c - I_b) = \Sigma_i m_i b_i^2$.
[19] M. D. Harmony, V. W. Laurie, R. L. Kuczkowski, R. H. Schwendeman, D. A. Ramsay, F. J. Lovas, W. J. Lafferty, and A. G. Maki, J. Chem. Phys. Ref. Data **8**, 619 (1979).
[20] J. Kraitchman, Am. J. Phys. **21**, 17 (1953).
[21] R. H. Schwendeman, *Critical Evaluation of Chemical and Physical Structural Information*, edited by D. R. Lide and M. A. Paul (National Academy of Sciences, Washington, DC, 1974), pp. 74–115.
[22] Landolt-Bornstein, *Zahlenwert und Funktionen* (Springer, Berlin, 1962), Vol. 2, Pt. 8, 871.
[23] J. M. Frisch, J. S. Binkley, H. B. Schlegel, K. Raghavachan, C. F. Melius, R. L. Martin, J. J. P. Stewart, F. W. Bobrowicz, C. M. Rohlfing, L. R. Kahn, D. J. DeFrees, R. A. Whiteside, D. J. Fox, E. M. Fluder, and J. A. Pople, GAUSSIAN86 (Carnegie-Mellon Quantum Chemistry Publishing Unit, Pittsburgh, PA, 1986).
[24] W. F. Murphy, J. Raman Spec. **11**, 339 (1981).
[25] W. Gordy and R. L. Cook, *Microwave Molecular Spectra*, 3rd ed. (Wiley, New York, 1984), p. 413.
[26] J. S. Muenter and R. L. DeLeon, J. Chem. Phys. **72**, 6020 (1980).
[27] N. Ramsey, American Scientist **49**, 509 (1961).
[28] M. R. Asdjodi, R. V. Gregory, G. C. Lickfield, H. G. Spencer, J. W. Huffman, and G. B. Savitsky, J. Chem. Phys. **86**, 1653 (1987).
[29] S. E. Emery, G. C. Lickfield, A. L. Beyerlein, and G. B. Savitsky, J. Mag. Res. **56**, 323 (1984).
[30] M. D. Marshall and W. Klemperer, J. Chem. Phys. **81**, 2928 (1984).
[31] R. L. DeLeon and J. S. Muenter, J. Mol. Spectrosc. **126**, 13 (1987).
[32] A simplified Hamiltonian was employed which neglects the effects of internal rotation on the A and C rotational constants. Thus, the estimates of splittings and barriers are only approximate. See Ref. 2 for additional discussions of the calculation.

[33]L. Pauling, *The Nature of the Chemical Bond* (Cornell University, Ithaca, 1960), p. 260.
[34]E. J. Goodwin and A. C. Legon, J. Chem. Phys. **85**, 6828 (1986).
[35]A. C. Legon, *Structure and Dynamics of Weakly Bound Molecular Complexes*, edited by A. Weber (Reidel, Dordrecht, Holland, 1987), pp. 23–42.
[36]D. J. Millen, Can. J. Chem. **63**, 1477 (1985). This equation is strictly correct only for $\theta = 0°$, where the C_2H_2 and SO_2 lie in parallel planes.
[37]W. G. Read and W. H. Flygare, J. Chem. Phys. **76**, 2238 (1982).
[38]J. A. Shea and W. H. Flygare, J. Chem. Phys. **76**, 4857 (1982).
[39]P. D. Aldrich, S. G. Kukolich, and E. J. Campbell, J. Chem. Phys. **78**, 3521 (1983).
[40]S. G. Kukolich, W. G. Read, and P. A. Aldrich, J. Chem. Phys. **78**, 3552 (1983).